Journal of Geosciences and Geomatics, 2022, Vol. 10, No. 3, 112-125
Available online at http://pubs.sciepub.com/jgg/10/3/1
Published by Science and Education Publishing
DOI:10.12691/jgg-10-3-1

Contribution to the Petrogenesis of Pan-Africain Granitoids from East Pitoa in the Northern Cameroon Domain of the Central Africain Fold Belt: Implications for Their Sources and Geological Setting

Cedric Roth Happi Djofna[1,*], Merlain Houketchang Bouyo[2], Daouda Dawai[3], Rigobert Tchameni[1], Landry Kouedjou[4], Martial Periclex Tchunte Fosso[1], Hervé Brice Fotso Kengne[1]

[1]Department of Earth Sciences, Faculty of Science, University of Ngaoundéré, P.O. Box 454, Ngaoundéré, Cameroon
[2]Centre for Geological and Mining Research, PO Box 333, Garoua, Cameroon
[3]Department of Earth Sciences, Faculty of Science, University of Maroua, P.O. Box 814, Maroua, Cameroon
[4]Department of Geography, Faculty Of Arts, Letters And Social Sciences, University of Ngaoundéré, P.O. Box 454, Ngaoundéré, Cameroon
*Corresponding author: happidjofna@yahoo.fr

Received May 11, 2022; Revised June 17, 2022; Accepted June 26, 2022

Abstract This article presents original geological and geochemical data on more or less deformed granitoids rocks of the Pitoa region in Domain North Cameroon. The Pitoa granitoids consist of leucocratic, gray and pink colored, fine to medium grained granites as well as quartz monzonite, containing numerous enclaves of mafic rocks, intruded in gneiss and amphibolite and cut by dykes of pegmatite, aplite and dolerite. They present porphyritic, inequigranular, granophyric and microgranophyric textures consisting essentially of quartz, K-feldspar, plagioclase, biotite and the accessory minerals are zircon, apatite, titanite and opaque minerals. The Plutonic rocks of Pitoa show the characteristics of the shoshonitic and calc-alkaline series with high-K content. They are magnesian to ferrous, luminous to slightly hyper-luminous metallic and exhibit the characteristics of type 1 granitoids. REE data and normalized chondritic plots show variable enrichment of all rocks in LREE compared to HREE with a negative europium anomaly (Eu/Eu*= 0.19 – 0.8), except for the pink granite sample DS15 which shows a positive Eu anomaly (14.6). They are distinctively depleted in Th, Nb, Ba, Sr, Ti and Ta. The data indicate that this assemblage of granitic rock did not result from the simple differentiation of a common parental magma, but show that the plutonic rocks of Pitoa arose from different crustal protoliths. Trace element and major composition are consistent with the magmatism which may have involved reworking of a composite protolith of metagrey-wackes in the upper crust and amphibolitised high -K calc-alkaline basaltic andesites in the northern domain of the Orogenic belt from Central Africa. These granitoids were set up in a tectonic context of continental subduction collision. They are emplaced in the active continental margin and fractional crystallization (FC) is a major process that controls magmatic differentiation.

Keywords: *petrography, geochemistry, north cameroon domain, pan-african granitoids, geodynamics*

Cite This Article: Cedric Roth Happi Djofna, Merlain Houketchang Bouyo, Daouda Dawai, Rigobert Tchameni, Landry Kouedjou, Martial Periclex Tchunte Fosso, and Hervé Brice Fotso Kengne, "Contribution to the Petrogenesis of Pan-Africain Granitoids from East Pitoa in the Northern Cameroon Domain of the Central Africain Fold Belt: Implications for Their Sources and Geological Setting." *Journal of Geosciences and Geomatics*, vol. 10, no. 3 (2022): 112-125. doi: 10.12691/jgg-10-3-1.

1. Introduction

Calco-alkaline granitoids are generally characterized by their hybrid petrographic aspect and their richness in enclaves. Their geochemical and isotopic compositions are intermediate between those of alkaline mantle granites and crustal leucogranites. These great characteristics reflect their mixed origin and their genesis by acid-base magmatic mixtures with the intervention of processes of crustal assimilation and fractional crystallization [1,2].

Also, the petrogenetic model of AFC (Assimilation Fractional Cristallization) developed by [3], has been widely accepted to explain the genesis of several calc-alkaline granitic plutons throughout the world [4,5]. Although the global model of the genesis of calc-alkaline granitoids seems well established, it turns out that each pluton has its own characteristics: distribution of granitic facies; nature; diversity of enclaves; magmatic evolution; and geochemical trend. This could be explained as much

by the diversity of the petrological processes that may occur simultaneously or in different orders as by the magmatic dynamic linked to the conditions of rise and establishment of the granitic magma which vary according to the geological context [6,7]. Also, each pluton constitutes a particular case whose analysis sheds light on a specific aspect of the petrogenesis of calc-alkaline granitoids. It is in this order of ideas that we have chosen to study the calc-alkaline granitoids of Pitoa. Moreover, with the exception of the geological reconnaissance work carried out by [8], the more or less deformed calc-alkaline granitoids of the eastern sector of Pitoa in particular have never been the subject of a detailed geological study. The integrated petrological and geochemical study of the main granite facies was carried out with the aim of characterizing the nature and origin of the various petrographic entities. This allowed us to clarify the relationships and interactions between them and therefore to reconstruct the history of the genesis of its granitoids.

2. Regional Geological Setting

The northern part of Cameroon (Figure 1), consists of (i) Neoproterozoic (~700 Ma) med- to high-grade Neoproterozoic shales and gneisses of the Poli-Léré group that formed in the context of a magmatic arc [9]; (ii) Pan-African pre-, syn- and late-tectonic calc-alkaline granitoids emplaced between 660 and 580 Ma [10,11]; (iii) post-tectonic alkaline granitoids including mafic and felsic dykes cross-cut by intrusive granites and syenites; followed by the formation of (iv) several basins made up of unmetamorphosed sediments and volcanic rocks [12,13].

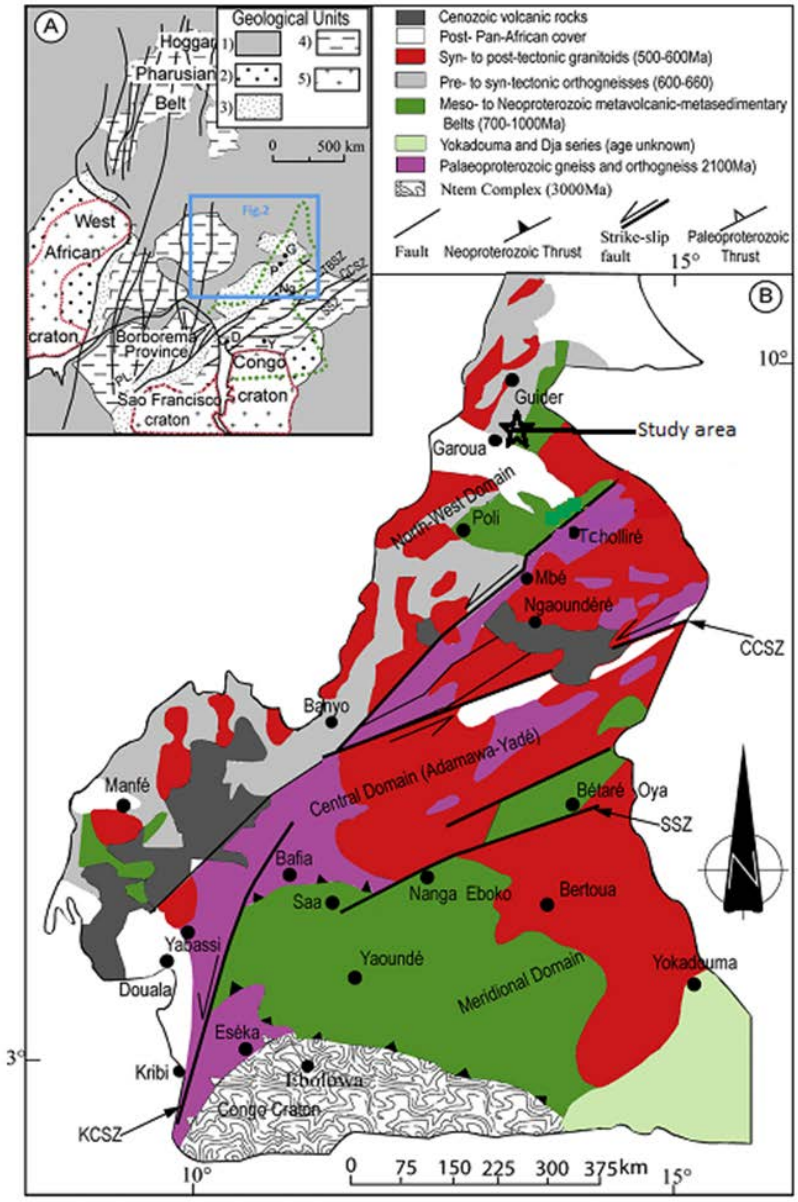

Figure 1. Geological context (A) Geology of West-central Africa and NE Brazil in a Gondwana (pre-drift) reconstruction modified from [10,19]. Dashed line boundary of Cameroon. Thick line, boundary of the two continents: (1) Phanerozoic cover; (2) Neoproterozoic formations; (3) Regions of Brasiliano/Pan-African deformation in which Paleoproterozoic basement is absent or only present as small isolated blocks; (4) Regions of Brasiliano/Pan-African deformation with large amounts of reworked Paleoproterozoic basement; (5) cratons. (B) Simplified geological map of Cameroon showing the location of the Pitoa area and major lithotectonic units. KCSZ = Kribi - Campo shear zone; CCSZ= Central Cameroon shear zone; SSZ=Sanaga shear zone; TBSZ =Tchollire-Banyo shear zone

Isotope dating indicates that most of the gneissic and granitic rocks in this domain are of Neoproterozoic age with a minor Palaeoproterozoic contribution, contrasting with the abundant Paleoproterozoic dating that characterizes the Adamawa-Yadé domain. This suggests that the Tcholliré-Banyo shear zone is a major boundary separating a juvenile Neoproterozoic upper crust on the west side, from older formations to the east [10,14].

Structurally, two deformation phases followed by late-orogenic shear zones are recorded in the NW-Cameroon domain, particularly in the Poli area [15,16] (Nzenti et al., 1992; Ngako et al., 2008). Flattened foliations associated with isoclinal folds and N110°–140° stretch lineations are locally well preserved. The second deformation is marked by vertical and NNE oriented foliations and by tight and upright folds. In this Poli area, syn-migmatitic N80°-N110° dextral and N160◦ –180◦ sinistral shear zones characterize to this second event. According to [17] the first event is attributed to crustal thickening and ended around 630-620 Ma. In the NW-Cameroon domain, the second event is characterized by left lateral (613-585 Ma) then by right lateral (585-540 Ma) tearing mouvements which controlled the emplacement of post-collision granitoids [16,18].

3. Methodology

For petrographic observations, polished thin slices of standard-size 27 × 46mm were prepared according to standard procedures. 25 x 40 mm sections of rock material were mounted with epoxy on carrier glass, covered with carborundum paper up to 2000 mesh to ~30 µm, and finished with diamond pastes 4-2-10.25µm on cloth to achieve a mirror finish.

For the geochemical analyses, rock powders were also obtained using standard methods. Geochemical analyses are carried out at Acmelabs in Canada. The prepared sample is mixed with the $LiBO_2/Li_2B_4O_7$ stream. The crucibles are melted in a furnace. The cooled bead is dissolved in ACS- grade nitric acid and analyzed by ICP and/or ICP-MS. Loss on ignition (LOI) is determined by igniting a fractionated sample and then measuring the loss in weight. Total Carbon and Sulfur can be included and are determined by the Leco method (TC003). The LF202 package includes 14 additional elements from an AQ200 aqua regia digestion to provide Au and volatile elements that are not part of the LF200 package.

4. Results

4.1. Field Data and Petrography

This study produced a geological map of Pitoa at a scale of 1: 50.000 including the sampling points (Figure 2). Two main types of lithology are observable: quartz monzonite and granite sensu stricto. They outcrop in slabs and metric to decametric blocks over several km in the localities of Badjouma Center and Badjouma radié. The vein rocks present in the area consist of gabbro, leucogranites, quartzo-feldspathic pegmatites and aplites. These vein rocks will be the subject of another study and will therefore not be studied in this work. The thin sections presented are those of the granites.

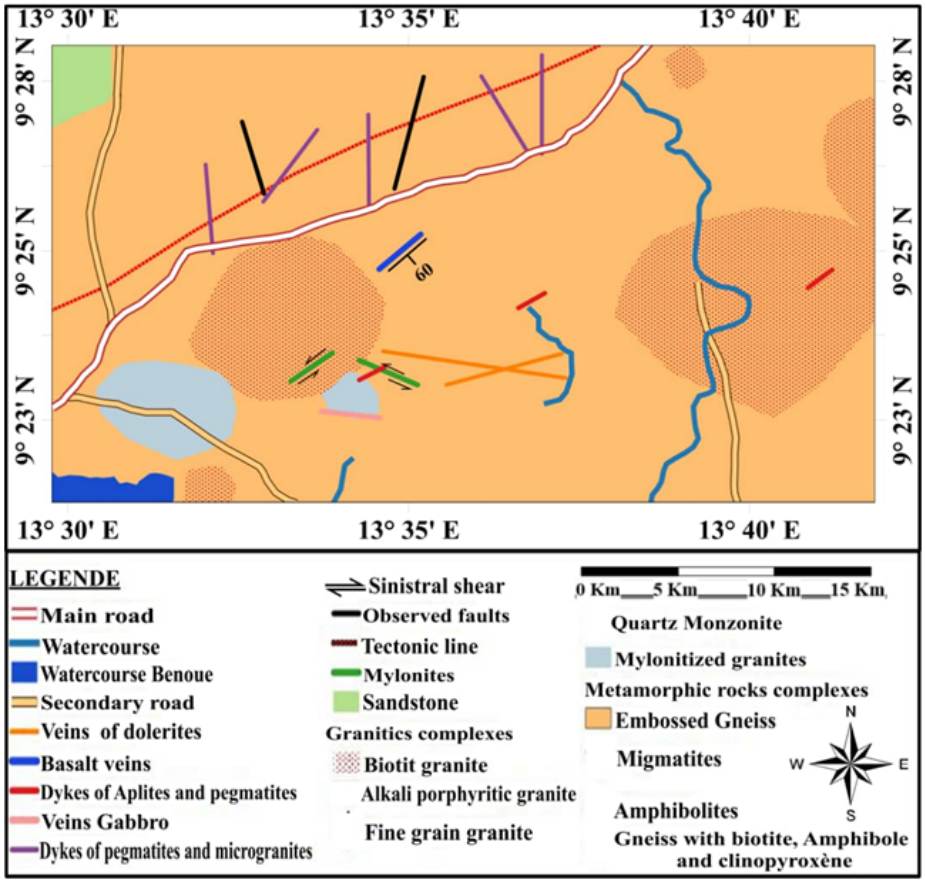

Figure 2. Geologic sketch map of the studied area

Figure 3. Some field observations of the studied rocks: (a) Block and slab outcrop of quartz monzonite, (b) Samples of quartz monzonite with coarse-grained texture, (c) porphyritic texture of the quartz monzonite showing associations of biotite, quartz and feldspar phenocrystals, (d) Highly billed granite flowing in a sheet that shows a preferential NE orientation, (e) Sample of the granite (deformed biotite granite), (f) photograph showing the protomylonitic to mylonitic texture in deformed biotite granite, (g) Stripe marked by alternating aplitic and grainy levels, (h) sample of granite (fine-grained biotite granite), (i) Fine-grained texture in biotite granite; (j)) Blocks of pink granite; (k) Sample of pink granite, (l) Pink granite with equant grained texture

4.1.1. Quartz Monzonite

They are represented in the field by coarse-grained biotite granites. The sample was collected near the Badjouma village (Figure 3a and b). It is light pink in color and has a coarse-grained texture. It is characterized by a porphyritic texture, consisting of plagioclase (showing fractures filled by sericite), K-feldspar, quartz phenocrysts and biotite. Opaque minerals are very low proportions and appear in the interstices of feldspars and biotite (Figure 3c).

4.1.2. Granite

Depending on the grain size, color, deformation and minerals, several types of granite are distinguished: deformed biotite granite, fine to medium-grained biotite granite and pink granite.

4.1.2.1. Deformed Biotite Granite

The deformed granite is a mylonitized granite outcropping in scattered or grouped blocks on the western flank of the massif (Mont Bayémi) and the village of Djaouro Sambo (Figure 3d). Highly fractured (cataclastic), the rock shows a preferential orientation towards the North. It is a fine-grained granite (Figure 3e) made up of millimeter-sized crystals (<1mm) of feldspar (K-feldspar, more abundant plagioclase), quartz, the rare biotite becoming chloritizing. At the microscopic scale, this sample shows a protomylonitic to mylonitic texture (Figure 3f) consisting of K-feldspar and plagioclase phenocrysts within a recrystallized groundmass made up of plagioclase, quartz, sericite, chlorite, zircon, rare small crystals of chloritized biotite and minor accessories minerals including epidote, apatite and oxide.

4.1.2.2. Fine Grained Biotite Granite

Fine-grained biotite granite outcrops near the Guebaké and Badjouma village. The rock outcrops in blocks and decametric slabs (Figure 3g). The slab presents bands marked by the alternation of aplitic levels. The rock is pinkish in color due to the abundance of K-feldspar

crystals, with a fine-grained structure (Figure 3h). Under the microscope, the texture is a fine-grained texture (Figure 3i), composed of quartz, plagioclase, K-feldspar and biotite. Secondary minerals are microcline, muscovite, sericite, calcite and opaque minerals. The essential minerals are millimeter-sized quartz and feldspar.

4.1.2.3. Pink Granite

Pink granite was collected near the village of Badjouma. The rock outcrops in blocks and decametric flagstone (Figure 3j). It is light pink in color and has an equant grain texture (Figure 3k). This variable-grained rock contains quartz and very abundant alkaline feldspar. Biotite and plagioclase are found in very small proportions in the rock. At the microscope scale, the texture is graphitic (Figure 3l), consisting of crystals of quartz (0.2 – 0.8mm), plagioclase, potassium feldspar and accessory minerals (calcite, zircon and opaque). These phenocrysts are embedded in an underground mass composed of quartz, feldspar, biotite and opaque minerals. Opaque minerals (5%) are included in quartz and feldspar crystals.

4.2. Geochemical Characterization

For geochemical studies, nine samples of granitic rocks were prepared. The sample weighing 0.5 to 1Kg was reduced and finely ground at the CRGM of Garoua (Geological and Mining Research Center of Garoua). The sample chips were cleaned, ground in an agate mortar, quarter split and finely ground. Representative samples were analyzed by ICP-AES and ICP-MS at "Acme Analytical Laboratories Ltd at Vancouver Canada".

4.2.1. Distribution of Major Elements

Major and trace element data for representative samples of granitoids are listed in Table 1. In the classification diagram of [20], the granitoids samples belong to the monzonite and QZ granite fields (Figure 4)

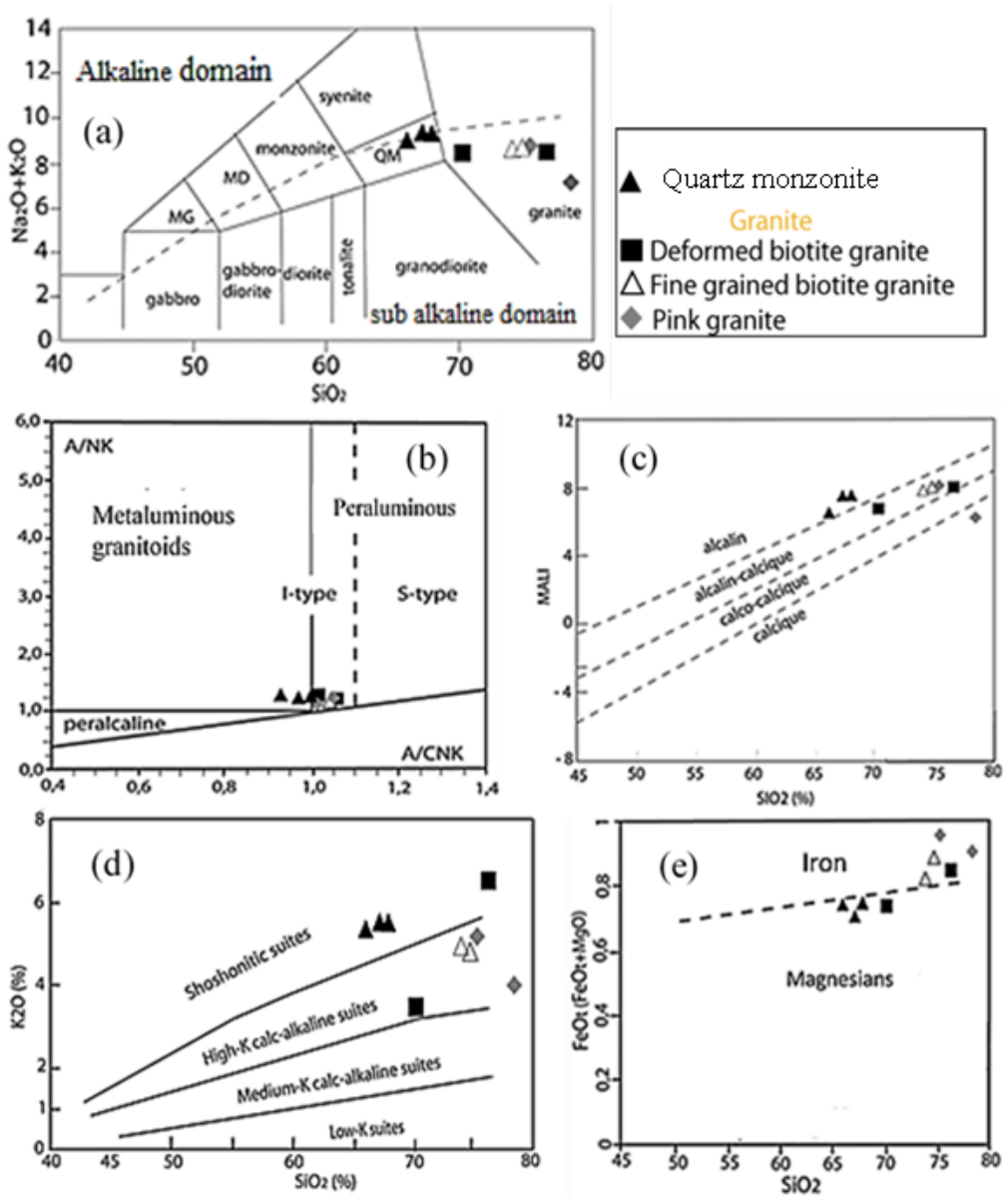

Figure 4. (a) $Na_2O + K_2O$ - SiO_2 diagram [20], the line dividing the alkaline domain from the calc-alkaline domain is after [29], (b) Diagram A/NK - A/CNK [21] showing the metaluminous to peraluminous nature of the plutonic rocks. (c) and (d) K2O-SiO2 (Peccerillo and Taylor, 1976) and Na2O+K2O-CaO-SiO2 [23] diagrams showing the calc-alkaline to shoshonite nature of the rocks studied. (e) FeO/MgO+FeO - SiO2 diagram [23] showing the magnesian and ferriferous nature of the Pitoa granitoïds

Table 1. Bulk-rock main element oxide (in wt%) and trace element contents (in ppm; µg·g-1ug/) measured by ICP and/or ICP-MS in representative plutonic samples from Pitoa

Rock type	Granites						Quartz monzonite		
Samples	DS01	DS15	BA03	PI01b	PI04	BC02	BC03	BR06	BC01
main element oxide contents and ignition loss in weight percent [wt%]									
SiO2	75.37	78.44	70.29	76.46	74.04	74.79	66.13	67.28	68.01
Al2O3	12.76	11.56	15.19	11.71	13.35	13.27	15.09	15.11	15.4
Fe2O3	1.35	0.91	1.84	1.69	1.78	1.47	4.02	3.22	2.94
MgO	0.05	0.08	0.61	0.29	0.36	0.18	1.23	1.22	0.86
CaO	0.64	0.88	1.69	0.57	0.79	0.67	2.48	1.84	1.79
Na2O	3.58	3.12	4.98	1.84	3.69	3.88	3.65	3.84	3.81
K2O	5.14	3.96	3.43	6.57	4.9	4.77	5.32	5.49	5.48
TiO2	0.09	0.04	0.26	0.16	0.18	0.16	0.69	0.53	0.44
P2O5	0.01	0.02	0.07	0.03	0.02	0.06	0.21	0.15	0.15
MnO	0.04	0.01	0.02	0.01	0.06	0.02	0.06	0.07	0.04
LOI	0.9	0.7	1.4	0.5	0.7	0.6	0.8	1	0.8
Total	99.92	99.72	99.78	99.83	99.87	99.87	99.68	99.75	99.72
CIPW NORME									
Quartz	33.13	43.19	23.49	38.59	31.12	32.04	16.81	17.45	19.18
Orthose	30.09	23.65	20.63	39.14	29.24	28.42	31.90	32.94	32.82
Albite	30.62	26.68	42.90	15.70	31.52	33.11	31.34	32.99	32.67
Anorthite	3.20	4.29	8.12	2.67	3.84	3.00	9.21	7.90	8.10
Magnétite	0.42	0.28	0.58	0.52	0.55	0.46	1.00	0.80	0.92
Ilménite	0,17	0.08	0.50	0.30	0.34	0.31	1.33	1.02	0.85
Corindon	0,14	0.59	0.37	0.60	0.59	0.64	0.00	-	0.27
Apatite	0,00	0.04	0.16	0.07	0.04	0.13	0.47	0.33	0.33
Na2O+K2O	8.72	7.08	8.41	8.41	8.59	8.65	8.97	9.33	9.29
K2O/Na2O	1.44	1.27	0.69	3.57	1.33	1.23	1.46	1.43	1.44
ANOR	9.46	15.36	28.20	6.39	11.60	9.53	22.40	19.34	19.81
Q'	33.91	44.15	24.70	40.16	32.51	33.17	18.83	19.11	20.68
Al/(Ca+Na+K) mol	1.01	1.05	1.00	1.05	1.04	1.04	0.93	0.97	1.00
Al/(Na+K) mol	1.11	1.23	1.28	1.15	1.17	1.15	1.28	1.23	1.26
trace element contents in partz per million [ppm; µg·g−1]									
Cr	ld	ld	ld	ld	ld	ld	27.37	61.58	ld
Ba	86	1542	758	588	269	120	838	1091	707
Ni	ld	ld	ld	ld	ld	ld	ld	ld	ld
Sc	3	ld	3.0	1	3	2	5	6	3
Be	6	ld	ld	ld	ld	6	3	5	4
Co	ld	0.7	2.2	1.4	0.8	1.7	7	4	5.2
Cs	4.5	0.6	2.5	0.2	0.5	5.9	7.8	2.9	7.1
Ga	20.4	10.9	21.1	15.3	17.6	18.5	19.5	18	17
Hf	5	5.6	3.5	7	2	4.6	10	7.6	6.6
Nb	26.2	0.5	3.3	5.4	10.2	9.7	23.5	17.2	14.4
Rb	367.6	69.2	88.7	149.4	129.6	291.1	245.2	185.2	271
Sn	4	ld	1.0	1	2	1	4	2	3
Sr	28.3	322	723.8	153.7	115.8	75.5	396.6	290.1	363.9
Ta	1.8	ld	0.3	ld	0.5	0.9	1.9	1.1	1.2
Th	63.9	0.5	7.0	26.4	6.7	44.7	54.6	20.1	41.5
U	7.9	0.3	2.1	0.8	0.5	12.5	8.2	3.2	6.6
V	ld	13	27.0	17	10	ld	50	27	31
W	1.3	ld	ld	ld	ld	ld	ld	ld	1.4
Zr	125	168.8	126.3	174.3	52.6	125.4	362.9	276.1	247.2
Y	24.7	1.5	6.5	16.4	9.4	6.2	19.5	20.5	12.7
Rb/Sr	12.99	0.21	0.12	0.97	1.12	3.86	0.62	0.64	0.74
Y/Sr	0.87	0.00	0.01	0.11	0.08	0.08	0.05	0.07	0.03
Nb/Zr	0.21	0.00	0.03	0.03	0.19	0.08	0.06	0.06	0.06
Rare Earth element contents in parts per million [ppm; µg·g−1]									
La	33.4	9.7	17.8	57.6	13.3	32.5	83.3	51.4	46.6
Ce	67.4	10.3	34.80	125.9	27.5	45.8	147.6	102.9	85.8
Pr	6.72	0.99	3.84	14.58	3.09	4.12	14.8	11.52	8.17
Nd	20.1	2.8	14.00	54.6	12	12.8	51.2	40.2	28.4
Sm	3.25	0.28	2.68	9.84	2.61	1.9	7.53	6.99	4.4
Eu	0.2	1.34	0.59	0.98	0.33	0.28	1.36	1.6	1
Gd	2.93	0.28	1.95	8.01	2.14	1.41	5.73	5.71	3.28
Tb	0.46	0.04	0.23	0.95	0.3	0.19	0.73	0.73	0.4
Dy	3.07	0.24	1.35	4.37	1.82	0.98	3.82	4	2.2
Ho	0.73	0.06	0.20	0.63	0.3	0.22	0.68	0.69	0.42
Er	2.39	0.25	0.70	1.44	0.9	0.64	2.04	2.03	1.22
Tm	0.47	0.03	0.09	0.18	0.11	0.09	0.28	0.28	0.17
Yb	3.79	0.24	0.59	1.1	0.86	0.73	1.85	1.91	1.17
Lu	0.66	0.06	0.09	0.17	0.13	0.14	0.29	0.28	0.19
ΣREE	145.57	26.61	78.9	280.35	65.39	101.8	321.21	230.24	183.4
(La/Yb)N	6.32	29.00	21.65	37.58	11.10	39.53	33.21	22.49	27.87
(La/Sm)N	6.64	22.39	4.29	3.78	3.29	11.05	7.15	4.75	6.84
(Dy/Yb)N	0.54	0.67	1.53	2.66	1.42	1.11	1.42	1.63	1.23
Eu/Eu*	0.19	14.6	0.74	0.34	0.42	0.52	0.63	0.78	0.8

Based on the Al saturation index (A/CNK = molar $Al_2O_3/(CaO + Na_2O + K_2O)$) of [21], the granites are peraluminous; quartz monzonites are distributed in the orefield and all conform to type-I granitoids (Figure 4a). In the MALI and K_2O vs SiO_2 diagrams, the granitoids show a calc- alkaline to shoshonitic trend and trace mainly in the domain of the high-K calc-alkaline series [22].

Using the classification of [23] to discriminate ferriferous granitoids from magnesian granitoids, the quartz-monzonites are magnesian and the granites are ferroian, except sample BA03 which is magnesian (Figure 4b, c et d). They present the same geochemical characteristics as those of the Mayo-Kebbi domain studied in the locality of Pala by [24] and those of the Adamaoua-Yadé domain mainly in the localities of Ngaounderé [25]; Meiganga [26]; Kékem [27] and Mbé-Sassa-Mbersi [28]. The SiO_2 vs oxide diagrams, of Harker type, show a quasi-linear and continuous distribution of points representing different petrographic facies of the plutonic rocks of Pitoa. This distribution established good negative correlations between SiO_2 and the other oxides (TiO_2, Al_2O_3, CaO, Fe_2O_3, MnO; P_2O_5, and MgO), and a random distribution for Na_2O and K_2O. Their contents decrease with the increase in the differentiation index expressed here by silica (Figure 5).

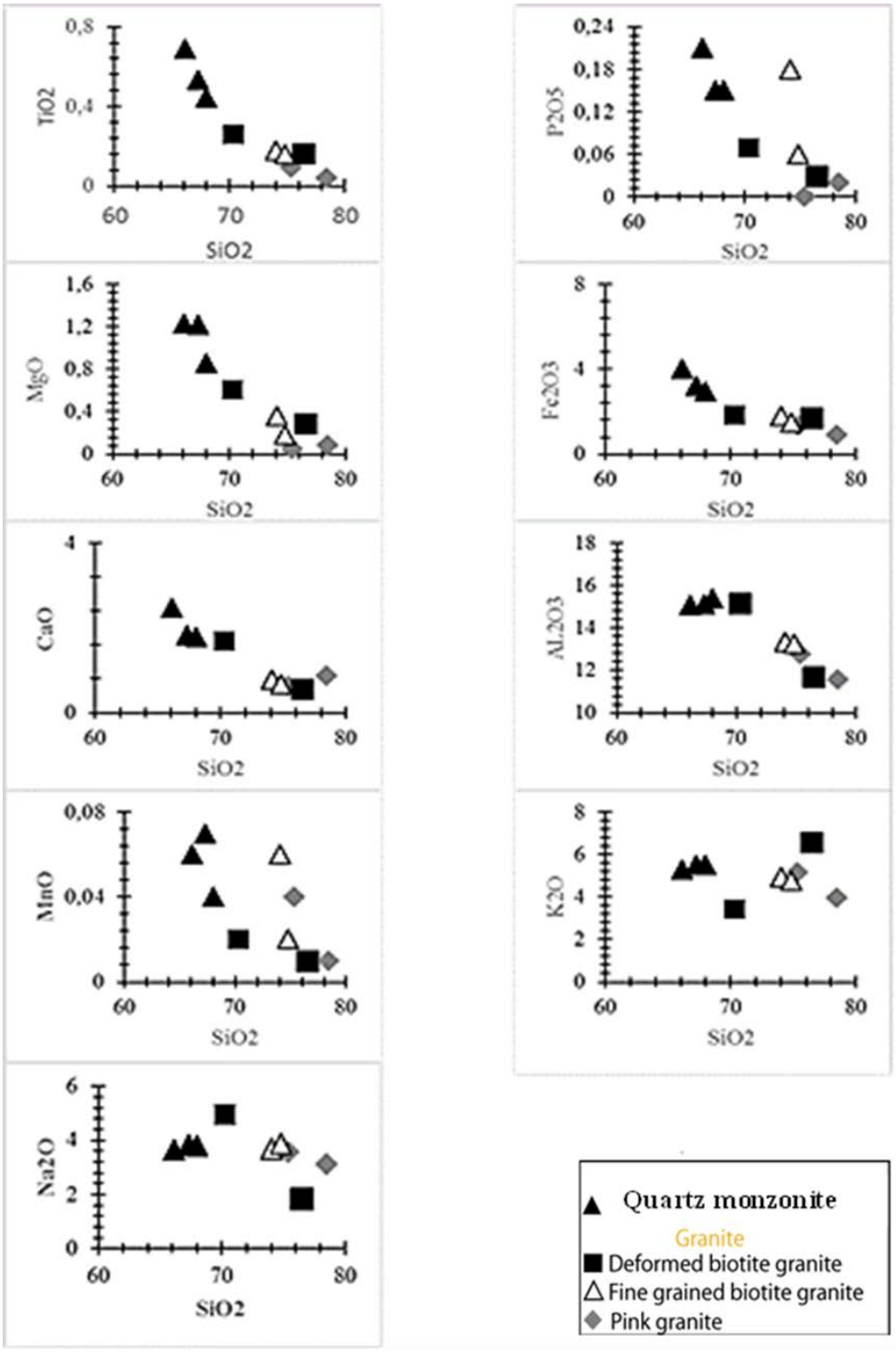

Figure 5. Harker diagram of Pitoa granitoids

4.2.2. Distribution of Trace Elements

4.2.2.1. Quartz Monzonite

Represented by the coarse-grained biotite granite on the field, they are characterized by high abundance of Ba (707 - 838ppm), Rb (271 – 245.2ppm), Sr (363.9 – 396.6ppm), Zr (247.2 – 362.9ppm) and Th (20.1 – 54.6ppm); moderate REE content (ΣREE =183.4 – 321.21ppm) and low Y content (12.7 – 19.5ppm). The Rb/Sr ratios vary from 0.62 to 0.74. Chondrite-normalized REE patterns (Figure 6a) are moderately fractionated (La_N/Yb_N= 28.58 – 33.21), and show negative Eu anomalies (Eu/Eu* = 0.63 – 0.8) and an HREE profile flat (Gd_N/Yb_N= 2.2 – 2.9). In the diagram of incompatible trace elements normalized by the Primitive mantle, the rocks show a homogeneous composition with strong negative anomalies in Ti (Ti_N/Gd_N= 0.3–0.4), P, Sr (Sr_N/Nd_N= 0.5 – 0.8), Nb (Nb_N/La_N= 0.3) and Ba (Figure 6b).

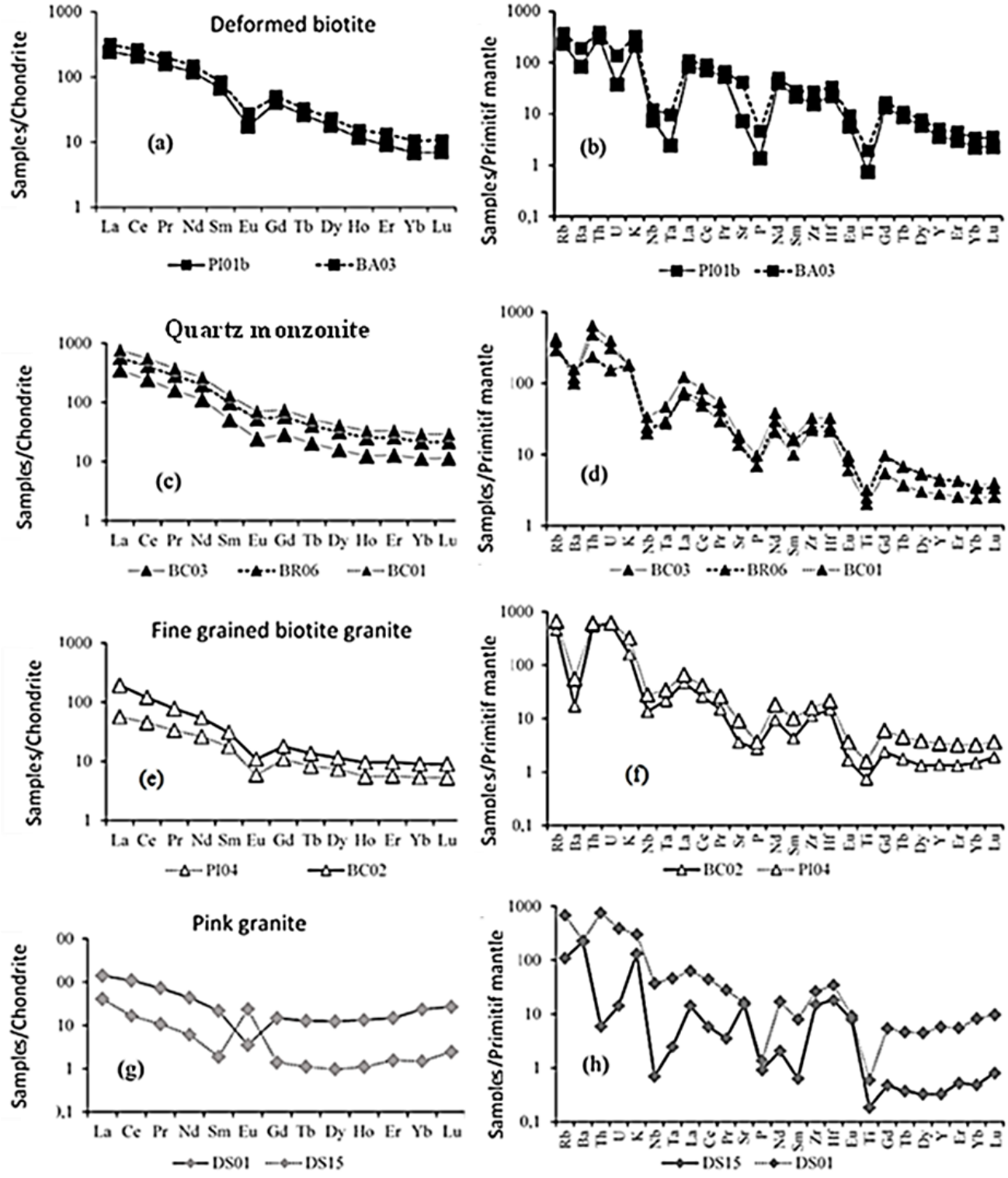

Figure 6. Chondritic-normalized REE patterns (a, c…) for the Pitoa granitoids. Normalizing values from [31]. Primitive mantle-normalized incompatible element patterns (idem) for the Pitoa granitoids. Normalizing values from [32]

4.2.3. Granites

4.2.3.1. Distorted Biotite Granite

The deformed biotite granite is characterized by high Ba contents (588 - 758ppm), Sr contents (153.7 – 723.8ppm), Th contents (26.4ppm, except sample BA03 with low concentration in Th, 7.0ppm), moderate in Rb (88.7 – 149.4ppm), Zr (126.3 – 174.3ppm) and REE (ΣREE =78.9 – 280.4ppm). The Rb/Sr ratios vary from 0.12 to 0.97. Chondrite-normalized REE models (Figure 6c) show enrichment in LREE relative to HREE (La_N/Yb_N= 2.65 – 37.58) and negative Eu anomalies (Eu/Eu*= 0.34 – 0.79). Compared to other Ngaoundéré granitoids, they are significantly depleted and fractionated in HREE (Gd_N/Yb_N= 2.73 – 6.02). In the primitive mantle-normalized incompatible element diagram (Figure 6d), all deformed biotite granite samples show patterns with negative Ba, U, Nb–Ta anomalies (Nb_N/La_N = 0.09 – 0.18), P and Ti (Ti_N/Gd_N= 0.05 – 0.37). Negative EU and BA anomalies are explained by the fractionation of plagioclase. But, Nb, Ta and some Ti negative anomalies are inherited from the petrogenetic process.

4.2.3.2. Fine-grained Biotite Granite

Fine-grained biotite granite is characterized by high Ba (120 – 1091ppm), low to moderate Rb (129.2 – 291.1ppm), Zr (52.6 – 276.1ppm), Sr (75.5 – 290.1ppm), Rare earths (ΣREE =65.39 – 230.24) and low Y contents (6.2 – 20.5ppm). The REE models normalized to Chondrite (Figure 6e) are moderately fractional (La_N/Yb_N= 11.09 –39.53), and have negative Eu anomalies (Eu/Eu* = 0.42 – 0.78) and a flat HREE profile (Gd_N/Yb_N= 1.6 – 2.9). In the normalized plot of the primitive mantle of incompatible trace elements, the rocks show a homogeneous composition with strong negative anomalies in Ba, U, Nb-Ta, P, Sm and Ti (Figure 6f).

4.2.3.3. Pink Granite

Pink granite is characterized by high Ba (1542ppm, except sample DS01 with low Ba concentration, 86ppm), Rb (367.6ppm, except sample DS15 with low Rb concentration, 69.2ppm), Zr (125 – 168.8ppm) and Sr (28.3 – 322ppm) contents. REE are low in these samples (ΣREE = 26.6 – 145.6ppm). The REE spectra of pink granites show common characteristics (Figure 6g). They are moderately fractionated ($(La / Yb)_N$ = 6.32 – 29) with heavy REE spectra concave upwards ($(Gd/Yb)_N$ = 0.63 – 0.94). Yb contents normalized to chondrites are generally variable (Yb_N = 1.50 – 23.54). The pink granite (DS01) shows a negative EU anomaly ((Eu/Eu* = 0.19)) while the DS15 sample shows a positive Eu anomaly ((Eu/Eu * = 14.6)). Multi-element spectra of pink granites are discordant. The spectra show negative Ba, Nb-Ta, P, Sm and Ti anomalies for sample DS01 while sample DS15 shows positive Ba, Sr anomalies and negative Th, Nb-Ta, Sm, Ti anomalies (Figure 6h).

5. Discussion

5.1. Source Rock Characteristics

The chemistry of granitic rocks is mostly controlled by the composition of the source. Granitoids can result either from fractional crystallization of mantle-derived magma or from partial melting of crustal rocks. Regarding the production of high-K magmas in convergent tectonic environments such as the Pan-African folded Belt in Cameroon, two main processes have been identified to explain: 1) in continental arc environments, fluid-enriched parent mantle magmas could be contaminated by crustal material during the ascent [33]; 2) in syn- to post-collisional environments, crustal rocks could melt as a result of post-peel decompression at the base of the lithosphere [34]. The differences in composition of the magmas produced by the partial melting of these different protoliths under varying melting conditions are illustrated in Figure 7a. In this diagram of [35], several observations can be made: i) The parental magmas of the studied plutonic rocks probably originated from a partial melting of a meta-greywacke source with a contribution of metabasic to tonalitic source ; ii) The magma of quartz monzonite (coarse-grained biotite granite) are mostly derived from partial melting of metabasic to tonalitic sources (except sample BC01 which derived from partial melting of metagreywacke) ; iii) Granitic magmas resulting from partial melting of a source of metagreywacke. Similar sources are found in the granitoids of eastern Nigeria and north eastern Brazil. These source rocks are predominantly found in the lower part of the continental crust and we suggest that the source of the quartz monzonite was metamorphosed mafic igneous rocks of the lower crust. The abundance of hydrous minerals (biotite) in the plutonic rocks suggests that the protolith melting took place under hydrous conditions. The differences observed in the granites can be explained by variations in the degree of mineral fractionation, differences in the melting conditions and/or minor variations in source compositions. The low Rb/Sr ratios (except sample DS01) and the LREE enrichment of the rocks are probably inherited from the source. As indicated by [36], the calc-alkaline to shoshonitic and metalluminous K-rich characters of the studied rocks involve a metalluminous and relatively K-enriched source. The metaluminous to weakly peraluminous feature as well as the presence of Magnetite and Sphene as main accessory minerals in the studied plutonic rocks suggest that their magma may have been formed by partial melting of a basic component according to [37]. The REE and multi-elements models in Figure 6 suggest genetic processes involving amphiboles and possibly garnets. High LREE contents in granites and quartz monzonites could be related either to LREE enrichment of their source materials or to a low degree of partial melting of crustal protoliths resulting in garnet and amphibole as residual phases. Moreover, the spider diagrams show no negative Y anomalies, suggesting that garnet was not involved in the residual phase. LREE enrichment, associated with HREE depletion during fractional crystallisation, is compatible with amphibole fractionation, which tends to concentrate HREEs. The heavy rare earth enrichment observed in pink granites reflects the presence of sphene and zircon in these rocks. Spider plots characteristically show negative anomalies for Ba, Nb and Ta. These anomalies result either from the low content of these elements in the source, or from their retention in the residue during partial melting. Thus, the magmatism of

the Pitoa plutonic rocks may have involved the reflow of a composite basic amphibolitic protolith into the deep crust. Low concentrations of Co, Ni and Cr are a geochemical characteristic of calc-alkaline granites of crustal origin. Large-scale melting of the source rocks may have been promoted by high heat flux during Pan-African Orogeny or under the plating of mantle derived magmas in the crust. In contrast, whole rock K/Rb ratios are relatively low in the quartz monzonite (136–180) and the sample of granite DS01 (116); moderate in granite (246–365, except for one sample, DS15 with 475), indicating highly evolved magma for the quartz monzonite and moderately evolved magma DS01 granite sample for other granites except sample DS15 which have a magmatic Figure 7b.

5.2. Magmatic Differentiation

The Pitoa plutonic rocks show a relative wide range of major and trace element compositions. Several processes could therefore be considered to explain their genesis, such as magmatic mixing and/or fractional crystallization.

5.2.1. Fractional Crystallization

The fractional crystallization process is well evidenced in the Harker diagrams. Straight curves symbolize the fractionation of a constant mineralogical assemblage, while breaks in slope generally indicate a change in the composition of the assemblage [40]. Graphs of selected major oxides Figure 5 shows well-defined negative or positive correlations with increasing SiO_2 content, which reveal the splitting of common mineral phases in granitic magmas. These rocks are characterized by a high SiO_2 content (66.13 - 78.44%) and incompatible elements suggesting a high degree of differentiation for the different granites studied. This differentiation is visible on the diagram FeOt / (FeOt + MgO) versus SiO_2 diagram (Figure 4**e**) with an increase in iron content compare to magnesium during differentiation. This increase in iron content during crystallization is due to the high degree of oxidative conditions in the magmas which promote the crystallization of iron oxides and which prevail in arc regions [40]. Plagioclase crystallization is confirmed by the negative Eu and Sr anomaly observed in the rare earth diagram (Figure 6). The Sr vs Ba diagram (not shown here) shows that magmatic differentiation in the biotite granites of Pitoa is controlled by alkali feldspar. Depletions of Ti, P, Sr, Ba, and Nb in the mantle-normalized primitive trace element patterns indicate the separation and crystallization of plagioclase, K-feldspar, apatite, ilmenite and others minerals (Figure 6). Within the pitoa granitoids in the northern domain of the Central African Orogenic belt, strong splitting of plagioclase, biotite, and K-feldspar is indicated by negative correlations of SiO_2 with CaO, Fe_2O_3, MgO, K_2O, MnO, Na_2O, P_2O_5 and Al_2O_3 (Figure 5). These features suggest that fractional crystallization played a major role in the magmatic process. According to [40], the fractional crystallization could be incomplete if the residual liquid (or part of it) remained trapped in the crystal matrix. This is generally reflected in our case by the presence of a protomylonitic texture in the deformed biotite granitoids marked by the presence of large phenocrysts molded by fine interstitial crystals. The Rb/Th Vs Rb diagram (Figure 8a) shows that several petrogenetic processes influenced the emplacement of the Pitoa granites, The Rb / Th Vs Rb diagram shows that several petrogenetic processes influenced the emplacement of the Pitoa granite, the major process is fractional crystallization and several criteria plead in favor of the intervention of the continental crust in the genesis of the intermediate and evolved terms present in the area.

5.2.2. Magma Mixing

In granitic terrains, the magmatic mixture is most often marked by the presence of dark enclaves of variable size [42,43]. The presence of these mafic enclaves of various shapes in the granitic slabs therefore seems to be a strong argument to suggest the intervention of such a process in the differentiation of the granitoids of the eastern sector of Pitoa (Figure 8c and d). Moreover, the progressive and unclear contacts between these enclaves and the granitic relief encountered in the field indicate a limited contamination of the enclave by the host and vice versa [42]. This process of magmatic mixing associated with fractional crystallization is observed in the granitoids of the Mbé –Sassa – Mbersi region by [28], granitoid rocks of the Mbengwi region by [43]. The role of mixing in the genesis of Pitoa plutonic rocks was further examined using the Yb/Hf ratio plotted against Ti/Zr (Figure 8b; e.g. [41]). The increasing linear correlations between these ratios are all expected characteristics for magma mixing.

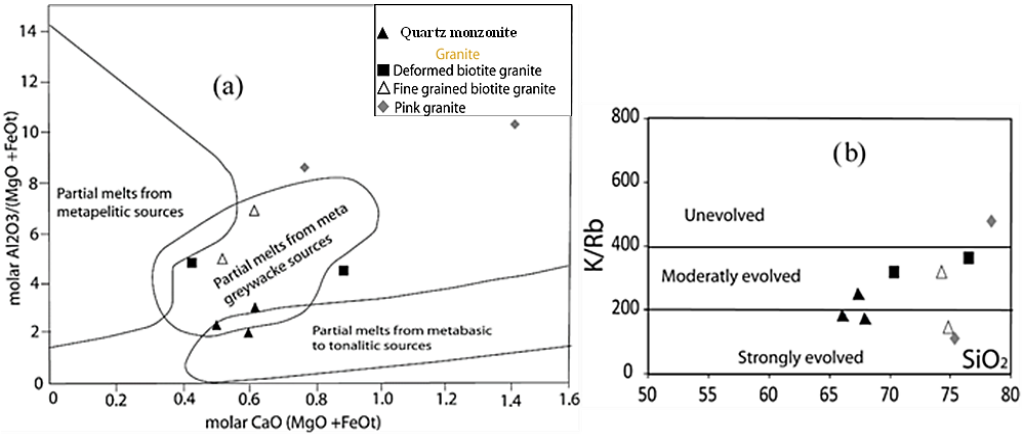

Figure 7. (a) Plots of the Pitoa granitoids in a molar Al_2O_3/(MgO + FeOt)–CaO/(MgO + FeOt) diagram [35], with composition fields of partial melts deriving from experimental dehydratation–melting of various source rocks [38]. (b) K/Rb vs. SiO2 diagram showing moderately to strongly evolved character of Pitoa granitoids after [39]

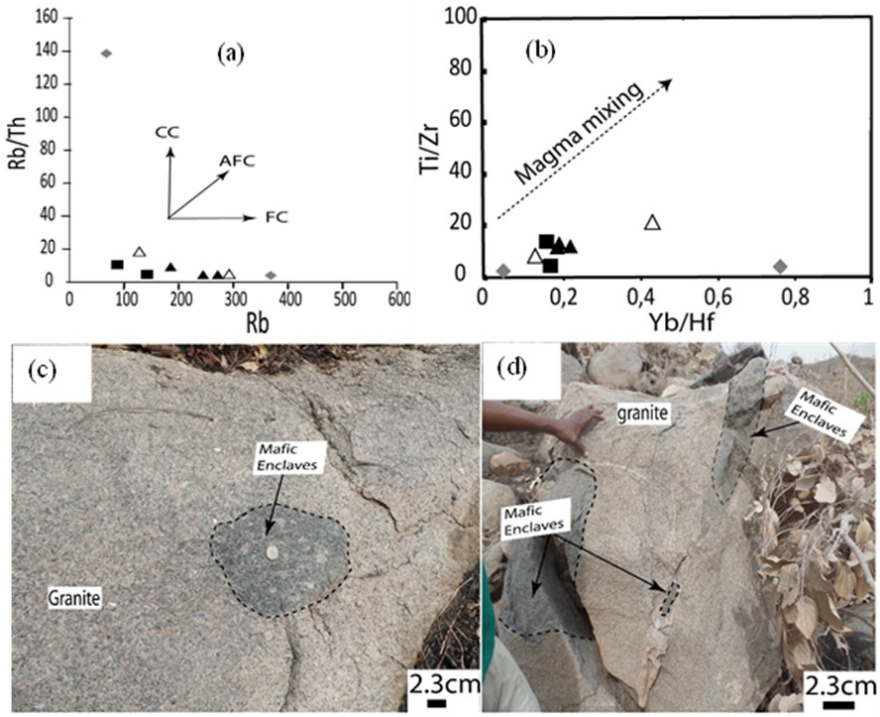

Figure 8. (a) Rb vs Rb/Th diagram for the Pitoa granitoids. AFC, assimilation–fractional crystallization; CC, crustal contamination; FC, fractional crystallization, (b) Ti/Zr vs. Yb/Hf diagram indicative magma mixing in the evolution of the studied rocks after [41]; (c) rounded mafic enclave in Badjouma biotite granite; (d) Mafic enclaves with elongated shapes in granite

5.2.3. Tectonic Settings and Tentative Geodynamic Context

The global geochemical characteristics of the Pitoa granitoids are compatible with the compositions of the calc-alkaline magmas of the orogenic domains. In the Yb vs Ta and the Y + Nb vs Rb discrimination diagram (Pearce et al., 1984; Figure 9a et b), the Pitoa granitoids clearly lie within the volcanic-arc granite field and are syn-collisional granites while the DS01 sample lies within the intra-plate granitic field. Pitoa granites are characterized by negative Ti, Nb, Ta and HREEs anomalies (Figure 6) characteristic of melting of oceanic and continental crust in subduction zones (e.g. [45]). The Ti anomaly suggests the crystallization of titano-magnetite oxides, and the abundance of iron oxides observed in the thin section would indicate a partial melting produced under oxidising conditions [46] within the lower crust. This abundance may reflect the melting of fluid and oxide-rich mantle material emanating from subducted oceanic lithosphere. Negative Nb-Ta anomalies can have several origins: petrogenesis associated with a subduction zone, strong crustal contamination or metasomatism of the mantle source [47]. The petrographic and geochemical data of the Pitoa granites argue in favor of a petrogenesis associated with a subduction zone. HREE depletion is also suggestive of refractory garnet at the magma source [48]. Negative anomalies in Zr and Hf also characterize certain rocks associated with subduction zones (White et al., 1984). On the Zr vs (Nb/Zr)N diagram (Figure 10) of [49], most of the samples trace fields from the collision zone to the subduction zones. These features and their high potassium calc-alkaline compositions are consistent with a continental collision context [12,50].

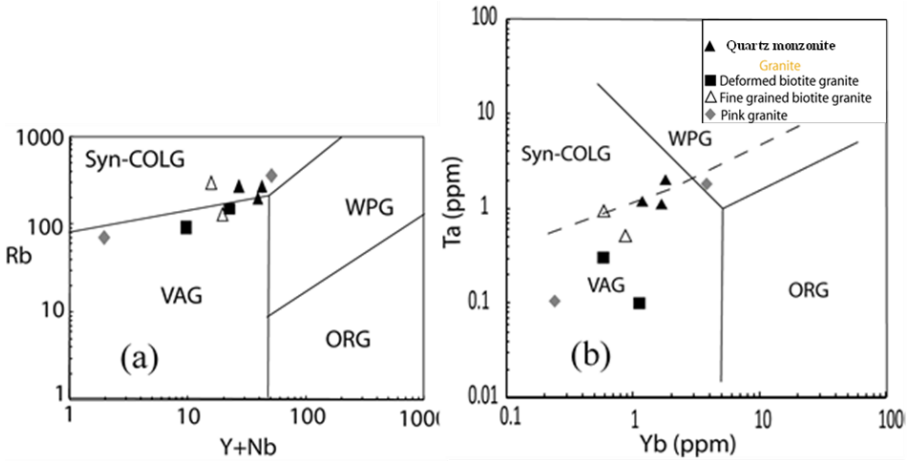

Figure 9. (a). (Y + Nb) vs Rb discrimination diagram and (b) Y vs Nb discrimination diagram for the Pitoa granitoids after [44]. Syn-COLG, syn-collision granite; VAG, volcanic arc granite; WPG, within-plate granite; ORG, ocean ridge granite

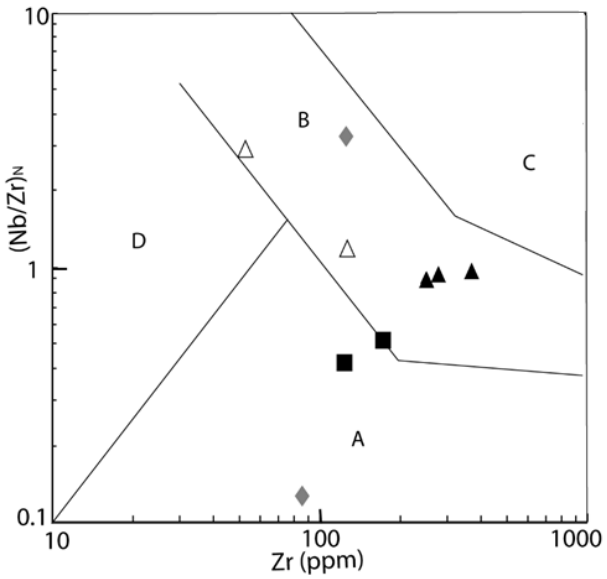

Figure 10. Zr vs (Nb/Zr)N diagram of Thiéblemont and Tegyey (1994) for the Pitoa granitoids: (A) subduction-zone magmatic rocks, (B) collision zone rocks; (C) alkaline intra-plate zone rocks; (D) Field of peraluminous leucogranites related to collision zones. Normalization values from Sun and McDonough (1989)

5.3. Relationship with Neighboring Domains

The North-Cameroon domain which extends to the Mayo kebbi [51,52] occupies a pivotal position between the formations of the East Nigeria domain and those of the Adamawa yadé domain. The geochemical studies carried out in this northern area on the syn-tectonic granites of the Guider and Bossoum-Pologozom plutons show trans-alkaline, meta-aluminous to hyper-aluminous characters on the one hand and ferro-potassium on the other hand [53]. These data made it possible to correlate them with the East-Nigeria and NE Brazil domains (Séridó Jaguaribe) which present the same geochemical characteristics [54,55]. The granitoids of the eastern sector of Pitoa located further south of Guider in the same area are slightly different. They are generally metalluminous to slightly hyperaluminous type I granites belonging to the calc-alkaline to high potassic shoshonite series. These granites tend to be much more ferriferous than magnesian and their silica content ranges from 66.13% to 78.44%. They present the same geochemical characteristics as those of the Mayo-Kebbi studied in the locality of Pala by [24,43] and those of the Adamaoua-Yadé domain mainly in the localities of Ngaounderé [25]; Meiganga [26]; Kékem [27] and Mbé-Sassa-Mbersi [28]. The same geochemical characteristics are also observed in the Pan-African granites of eastern Nigeria, emplaced during a collision-subduction of the eastern edge of the West African craton [56]. The approximately linear distribution of Pitoa granitoids in Harker diagrams and the presence of mafic enclaves in the granite would indicate the intervention of magmatic mixing (acidic and basic magma) as well as fractional crystallization processes [57,58]. Two magmatic processes are also highlighted in the Mbé – Sassa - Mbersi granitoids (Saha et al., 2019) [28]. The multi-element spectra show all the negative anomalies in Nb-Ta and TiO_2, reflecting the presence of a crustal component in the parent magma linked either to a mantle modified by subduction phenomena, or to crustal contamination during their setting in place. The Pitoa granitoids are established in contexts of active continental margins just like those of Mbé - Sassa-Mbersi. They are all syn-collisional volcanic arc granitoids resulting from a multi-source magma (melting plunging plate, upper continental crust, and magmatic mixture) placed in a situation of subduction-continental collision. Fractional crystallization (FC), assimilation by fractional crystallization (AFC), and magmatic differentiation controlled by crustal contamination (CC).

6. Conclusions

The aim of this study was to identify the lithologies of Pitoa and their emplacement conditions emplacement. To achieve these objectives, petrographic, and geochemical characterizations were necessary. The main results show that the Pitoa zone is made up of quartz monzonite and granites with porphyritic, inequigranular, granophyric and microgranophyric textures. They are composed of quartz, feldspars (plagioclase and K-feldspar) and biotite. Muscovite and calcite are secondary minerals. Accessory minerals are epidote, apatite, zircon and opaque minerals.

The Pan-African Pitoa granitoids are calc-alkaline, high K, I-type and metaluminous to peraluminous that are related to the rocks of Mbengwi, Mbé-Sassa-Mbersi and Ngaounderé. Differences in these granitoid groups can be explained by variations in source composition, melting conditions and degree of mineral fractionation. They are syn-collisional volcanic arc granitoids resulting from a multi-source magma (molting plunging plate, upper continental crust and magmatic mixture) placed in subduction – continental collision.

Fractional crystallization played a major role in the magmatic process.

Acknowledgements

This manuscript is a part of the thesis of the first author co-supervised between the University of Ngaoundéré (Cameroon) and the Geological and Mining Research Center of Garoua. The authors acknowledge the constructive comments of the anonymous reviewers and are also grateful to the editors for the diligent editorial management of the manuscript.

References

[1] Pin, C., Binon, M., Belin, J.M., Barbarin, B. & Clemens, J.D. 1990: Origin of microgranular enclaves in granitoids: Equivocal Sr-Nd evidence from Hercynian rocks in the Massif Central (France). *J. Geoph. Res.* 95, 17, 821-17, 828.

[2] Donaire, T., Pascual, E., Pin, C. & Duthou, J-L. 1999: Tow-stage granitoid-forming event from an isotopically homogeneous crustal source: The Los Pedroches batholith, Iberian Massif, Spain. *GSA Bull*. V. 111, 12, 1897-1906.

[3] Depaolo, D.J. 1981: Trace element and isotopic effects of combined wallrock assimilation and fractional crystallization. *Earth Plant. Sci. Lett.* 53, 189-202.

[4] Barbarin 1989: Importance des différents processus d'hybridation dans les plutons granitiques du batholite de la Sierra Nevada, Californie. Schweiz.Mineral. *Petrogr. Mitt.* 69, 303-315.

[5] Roberts, M.P., Pin, C., Clemens, J. D. & Paquette, J.L. 2000: Petrogenesis of Mafic to Felsic Plutonic Rock Association: the Calc-alkaline Quérigut complex, Franch Pyrenees. *J. Petrol*. 41, 809-844.

[6] Huppert, H.E. & Sparks, R.S.J. 1988: The generation of granitic magmas by intrusion of basalt into continental crust. *J. Petrol*. 29, 599-624.

[7] Johannes, W. & Holtz, F. 1991: Formation and ascent of granitic magmas. *Geol. Rdsch*. 80, 225-231.

[8] schwoerer, P., 1965. Notice explicative sur la feuille de Garoua Est avec une carte géologique de reconnaissance au 1/500000. Direction des mines et géologie, Yaoundé, 49p. Imprimerie Nationale Yaoundé.

[9] Toteu, S.F., Yongue Fouateu, R., Penaye, J., Tchakounté, J., Seme Mouangue, A.C., Van Schmus, W.R., Deloule, E., Stendal, H., 2006a. U-Pb dating of plutonic rocks involved in the nappe tectonic in southern Cameroon: consequence for the Pan-African orogenic evolution of the central African fold belt. *J. Afr. Earth Sci*. 44, 479-493.

[10] Toteu S.F., Van Schmus W.R., Penaye J., Michard A., 2001. New U-Pb and Sm-Nd data from north-central Cameroon and its bearing on pre-Pan-African history of central Africa. *Precambrian Res*. 108, 45-73.

[11] Penaye, J., Kröner, A., Toteu, S.F., Van Schmus, W.R., Doumnang, J.C., 2006. Evolution of the Mayo Kebbi region as revealed by zircon dating: an early (ca. 740 Ma) Pan-African magmatic arc in south western Chad. *J. Afr. Earth Sci*. 44, 530-542.

[12] Toteu, S.F., Penaye, J., Poudjom Djomani, Y., 2004. Geodynamic evolution of the Pan-African belt in Central Africa with special reference to Cameroon. *Canadian Journal Earth Sciences* 41, 73-85.

[13] Van Schmus W. R., Oliveira E. P., da Silva Filho. A. F., Toteu S. F., Penaye J., Guimarães I. P., 2008. Proterozoïc links between the Borborema Province, NE Brazil, and the Central African Fold Belt. *Geological Society, London, special Publications;* v. 294, pp 69-99.

[14] Bouyo Houketchang, M., Toteu, S.F., Deloule, E., Penaye, J., Van Schmus, W.R., 2009. U–Pb and Sm–Nd dating of high-pressure granulites from Tcholliré and Banyo regions: evidence for a Pan-African granulite facies metamorphism in northcentral Cameroon. *Journal of African Earth Sciences* 54, 144-154.

[15] Nzenti, J.P., Ngako, V., Kambou, R., Penaye, J., Bassahak, J., Njell, O.U., 1992. Structures régionales de la chaîne panafricaine du Nord Cameroun: *Comptes Rendus Académie des Sciences Paris*, série II 315, 209-215.

[16] Ngako V., Affaton P., Njonfang E., 2008. Pan-African tectonics in northwestern Cameroon: implications for the history of western Gondwana. *International Association for Gondwana Research* 14: 509-522.

[17] Ngako, V. and Njonfang, E., 2011. Plates amalgamation and plate destruction, the Western Gondwana history. In: D. Closson (Ed.), Tectonics. *INTECH, UK*, p. 3-34.

[18] Njanko, T., Nédélec, A., Kwékam, M., Siqueira, R., Estéban, L., 2010. Emplacement and deformation of the Fomopéa pluton: implication for the Pan-African history of Western Cameroon. *Journal of Structural Geology* 32, 306-320.

[19] Castaing, C., Feybesse, J.-L., Thiéblemont, D., Triboulet, C., Chèvremont, P., 1994. Paleogeographical reconstructions of the Pan-African/Brasiliano orogen: closure of an oceanic domain or intracontinental convergence between major blocks. *Precambrian Research* 69, 327-344.

[20] Lebas, M.J., Le Maitre, R.W., Strecksein, A., Zanettin, B., 1986. A chemical classification of volcanic rocks based on the total alkali- silica diagram. *Journal of petrology* 27, 745-750.

[21] Shand, S.J., 1943. Eruptive Rocks. Their Genesis, Composition, Classification, and Their Relations to Ore-deposits. Wiley, New York 444 pp.

[22] Peccerillo A., Taylor S. R., 1976. Geochemistry of Eocene cal-alkaline volcanic rocks from the Kastamonu area, northern Turkey. Contributions to Mineralogy and Petrology 58: 63-81.

[23] Frost, B.R., Barnes, C.G., Collins, W.J., Arculus, R.J., Ellis, D.J., Frost, C.D., 2001. A geochemical classification for granitic rocks. *J. Petrol*. 42 (11), 2033-2048.

[24] Pouclet, A., Vidal, M., Doumnang, J.C., Vicat, J.-P., Tchameni, R., 2006. Neoproterozoic evolution in the Southern Chad: Pan-African Ocean basin closing, arc accretion and late- to post-orogenic granitic intrusion. *J. Afr. Earth Sci.* 44, 543-560.

[25] Tchameni R., Pouclet A., Penaye J., Ganwa A. A., Toteu S. F., 2006. Petrography and geochemistry of the Ngaoundéré Pan-African granitoïds in central North Cameroon: implications for their sources and geological setting, *J. African Earth Sci.*, 44: 511-529.

[26] Ganwa A.A., Siebel W., Frisch W., Shang C.K., 2011. Geochemistry of magmatic rocks and time constraints on deformational phases and shear zone slip in the Meiganga area, central Cameroon. *Int. Geol. Rev*. 53, 759-784.

[27] Kwekam M., Liegeois J.P., Njonfang E., Affaton P., Hartmann G., Tchoua F., 2010. Nature, origin and significance of the Pan-African high-K calc-alkaline Fomopea plutonic complex in the Central African fold belt (Cameroon). *J. Afr. Earth Sci*. 57, 79-95.

[28] Saha-Fouotsa Alliance Nicaise, Olivier Vanderhaeghe, Pierre Barbey, Aurélien Eglinger, Rigobert Tchameni, Armin Zeh, Periclex Fosso Tchunte, Emmanuel Negue Nomo., 2019. The geologic record of the exhumed root of the Central African Orogenic Belt in the central Cameroon domain (Mbé–Sassa-Mbersi region). *Journal of Earth Science.*

[29] Irvine, T. N. & W. R. A. Baragar 1971. A guide to the chemical classification of the common rocks. Can. *J. Earth Sci*. 8, 523-48.

[30] Harker, A. 1909. The natural history of igneous rocks. New York: Macmillan.

[31] Mc Donough WF, Sun SS. 1995. The composition of the Earth. *Chemical Geology*, 120: 223-253.

[32] Sun, S.-S., McDonough, W.F., 1989. Chemical and isotopic systematics of oceanic basalts: implications for mantle composition and processes. In: In: Saunders, A.D., Norry, M.J. (Eds.), Magmatism in the Ocean Basins, vol 42. *Geol. Soc. London Spec. Publ*., pp. 313-345.

[33] DePaolo, D.J., 1981. A neodymium and strontium isotopic study of the Mesozoic calc-alkaline granitic batholiths of the Sierra Nevada and Peninsular Ranges, california. *Journal of geophysic Research* 86, 10470-10488.

[34] Liégeois et al., 1994 J.P. Liégeois, R. Black, J. Navez and L. Latouche, Early and late PanAfrican orogenies in the Aïr assembly of terrane (Tuareg shield, Niger), *Precambrian Research* 67 (1994), pp. 59-88.

[35] Altheer R., Holl A., Hegner E., Langer C., Kreuzer H., 2000. High potassium, calc-alkaline I-type plutonism in the European Variscides: northern Vosges (France) and northern Schwarzwald (Germany). *Lithos* 50: 51-73.

[36] Roberts, M.P. and Clemens, J.D. (1993) Origin of High-Potassium, Talc-Alkaline, I-Type Granitoids. *Geology*, 21, 825-828.

[37] Chappell, B.W., White, A.J.R. 1974. Two contrasting granite types. *Pacific Geology* 8, 173-174.

[38] Partino D. A. E., Beard J. S., 1996. Effects of P, f (O2) and Mg/Fe ratio on deshydratation melting of model metagrauwackes. *Journal of Petrology* 37: 999-1024.

[39] Blevin, P. L. (2004). Redox and composional parameters for interpretating the granitoid metallogeny of Eastern Austria: implications for gold-rich ore system. *Resour. Geol.* 54, 241-252.

[40] Bonin, B., Moyen, J.F., Magmatisme et roches magmatiques, 3e édition, *Dunod, Paris*, 2011.

[41] Aydoğan, M.S., Coban, H., Bozcu, M., Akinci, Ö., "Geochemical and mantle-like isotopic (Nd, Sr) composition of the Baklan Granite from the Muratdağı Region (Banaz, Uşak), western Turkey: Implications for input of juvenile magmas in the source domains of western Anatolia Eocene-Miocene granites", *J Asian Earth Sci*, 33, 155-176, 2008.

[42] Nedelec A., Bouchez J.-L., 2015. Granites: Petrology, Structure, Geological Setting and Metallogeny. *Oxford University Press*, p. 335.

[43] Benoît Joseph Mbassa, Emmanuel Njonfang, Caroline Neh Ngwa, Michel Grégoire, Zénon Itiga, Pierre Kamgang, Mfomou Ntepe, Jesús Solé Viñas, Mathieu Benoit, Jacques Dili-Rake, and Ferdinand Mbossi Eddy, "Mineral Chemistry and Descriptive Petrology of the Pan-African High-K Granitoids and Associated Mafic Rocks from Mbengwi, NW Cameroon: Petrogenetic Constraints and Geodynamic Setting." *Journal of Geosciences and Geomatics*, vol. 8, no. 2 (2020): 58-75.

[44] Pearce J. A., Harris N. W., Tindle A. G., 1984. Trace element discrimination diagrams for the tectonic interpretation of granitic rocks. *Journal of Petrology* 25: 956-983.

[45] Thirlwall M. F., Smith T. E., Graham A. M., Theodorou N., Hollings P., Davidson J.P., Arculus R .J., 1994. High field strength element anomalies in arc lavas: Source or process? *Journal of Petrology*, v. 35, p. 819-838.

[46] Ishihara S., 1977. The magnetite-series and ilmenite-series granitic rocks: *Mining Geology*, v. 27, p. 293-305.

[47] Guy Scherrer., 2003. Géochimie et pétrogenèse des roches métagabbroiques du domaine du Natashquan secteur oriental de la province de Grenville, Québec. Mémoire pour obtention du grade de maître des sciences en science de la terre. Université de québec.121p+Annexes.

[48] Rollinson H. R., 1993. Using Geochemical Data: Evaluation, Presentation, Interpretation. Longman Scientific & Technical co published in the United States with John Wiley & Sons, New York. 351 pages.

[49] Thiéblemont D., Tegyey M., 1994. Une discrimination géochimique des roches différenciées témoin de la diversité d'origine et de situation tectonique des magmas calco-alcalins. *Comptes Rendus de l'Académie des Sciences Paris* 319: 87-94.

[50] Liégeois, J.-P., Navez, J., Hertogen, J., and Black, R. (1998). Contrasting origin of post-collisional high-K calc-alkaline and shoshonotic versus alkaline and peralkaline granitoids. The use of sliding normalization. *Lithos* 45, 1-28.

[51] Bouyo, M.H., Penaye, J., Njel, U.O., Moussango, A.P.I., Sep, J.P.N., Nyama, B.A., Wassouo, W.J., Abate, J.M.E., Yaya, F., Mahamat, A., Ye, H., Wu, F., 2016. Geochronological, geochemical and mineralogical constraints of emplacement depth of TTG suite from the Sinassi Batholith in the Central African Fold Belt (CAFB) of northern Cameroon: implications for tectonomagmatic evolution. *J. Afr. Earth Sci.*116, 9-41.

[52] Emmanuel Negue Nomo., Rigobert Tchameni., Olivier Vanderhaeghe., Fenguye Sun c., Pierre Barbey., Leontine Tekoum., Periclex Martial Fosso Tchunte., Aurelien Eglinger., Nicaise Alliance Saha Fouotsa., 2017. Structure and LA-ICP-MS zircon U-Pb dating of syntectonic plutons emplaced in the Pan-African Banyo-Tchollire shear zone (central north Cameroon). *Journal of African Earth Sciences* 131 (2017) 251-271

[53] Dawaï, D., Bouchez, J.L., Paquette, J.L., Tchameni, R., 2013. The Pan-African quartzsyenite of Guider (North-Cameroon): magnetic fabric and U-Pb dating of the late-orogenic emplacement. *Precambr. Res*. 236, 132 -144.

[54] Nascimento M.A.L., Antunes A.F., Galindo A.C., Jardim de Sa E.F., Souza Z.S., 2000. Geochemical signature of the brasiliano-age plutonism in the serido belt, northeastern Borborema Province (NE Brazil). *Rev. Bras. Geociências* 30, 161-164.

[55] Guimaraes I.P., Da Silva Filho A.F., Araújo D.B., Almeida C.N., Dantas E.L., 2009. Trans-alkaline magmatism in the serrinhaepedro velho complex, Borborema Province, NE Brazil and its correlations with the magmatism in eastern Nigeria. *Gondwana Res.* 15, 98-110.

[56] Kwékam, M., Genèse et évolution des granitoïdes calco-alcalins au cours de la tectonique panafricaine: le cas des massifs syn à tardi-tectoniques de l'Ouest-Cameroun (Régions de Dschang et de Kekem), Thèse Doct d'État, Univ Yaoundé I, 2005.

[57] Orsini J.B., Cocirta C. & Zorpi M.J. 1991. Genesis of mafic microgranular enclaves trough differenciation of basic magmas, mingling and chemical exchanges with their host granitoid magmas. In: Didier J. & Barbarin B. (eds) Enclaves and granite petrology, Develop. Petrol. 13, *Elsevier*, 445-463.

[58] Boukaoud E. H., 2007. Étude pétrographique et géochimique des pegmatites de Sidi Mezghiche (Wilaya de Skikda, nord-est algérien). Mémoire de magistère, université Mentouri Constantine, Algérie, 134p.